ORIGINAL ARTICLE

Simple Push-Type Wave Generating Method Using Digital Rotary Valve Control

Yi Liu[1,2], Jiafei Zheng[1,3], Ruiyin Song[1,2*], Qiaoning Xu[4], Junhua Chen[1,2] and Fangping Huang[1,2]

Abstract

The important parameters to describe waves are their amplitude and length. In order to make it easier to improve wave amplitude and facilitate wave experiment, a simple push-type wave generating method using digital rotary valve control was proposed and different wave amplitudes were generated by the new method. After the mathematical model of the new method had been established, numerical analysis based on the linear wave theory was carried out by means of Matlab/Simulink software tools, and experiments were conducted on the push-type wave maker to ascertain the validity of the established model and the numerical simulation results. It shows that both experimental and theoretical results agree relatively well, and the plate motion frequency and amplitude of the push-type wave maker can be continuously adjusted and the various required regular waves can be obtained. Although the wave amplitude and length descends with the increasing of working frequency, the wave amplitude can be improved conveniently by setting the axial opening width of the valve and the oil supply pressure of system. The wave length remains unchanged with the axial opening width and the oil supply pressure change. The research indicates that different regular waves can be easily generated by the new method and the wave amplitude can be further improved in a certain plate motion frequency range.

Keywords: Push-type wave maker, Digital rotary valve control, Mathematical modeling, Wave amplitude, Wave frequency

1 Introduction

The wave maker is one of the most important facilities in the research field of ocean engineering and hydraulic engineering. Its performance of wave simulation has an effect on the testing of sea keeping. As the wave maker plays an extremely important role in engineering research, the theory and implementation of wave generation have been attracting extensive attention for years. Scientists often perform laboratory experiments on the basis of push-type wave makers, which move a wave plate to generate waves [1, 2]. Refs. [3, 4] facilitates the generation of arbitrary finite-amplitude waves at any distance from the wave maker. Moronkeji [5] performed experimental studies using electrically driven wave plates

to improve plate amplitude. Teng et al. [6] reported a variation of the commonly used push-type wave maker principle. By varying the speed and distance between the carriage and plate, waves of different amplitudes were generated. This method resolved the problem related to limiting the plate amplitude of push-type wave makers. The study of Wu et al. [7] on long waves generated by a push-type wave maker concludes that the method proposed by Wu et al. [8] was effective for generating solitary waves of stable height. The technology of generating white noise wave requires that wave amplitudes remain stable in a certain plate frequency range. White noise wave spectrum is basically flat in the floating objects test and this technology makes frequency response function more reliable in experiment analysis in a large frequency range [9].

The wave generator driven by electric motor is widely used in low load; for example, rocker flap wave maker. Conversely, the hydraulic wave generator could produce

*Correspondence: ruiyinsong@163.com
[1] Ningbo Institute of Technology, Zhejiang University, Ningbo 315100, China
Full list of author information is available at the end of the article

Liu *et al. Chin. J. Mech. Eng.* (2020) 33:5

Page 2 of 11

high torque with quick-response and high-accuracy, thus it can be applied in push-type wave maker in heavy load. Electro-hydraulic servo technology was frequently adopted as a solution of high-power and high-accuracy vibration systems in recent years [10, 11]. To obtain the high flow, thrust, and frequency in these driving systems, a variety of electro-hydraulic excitation devices with high thrust and high frequency were studied by many scholars, as a result, the AC servo hydraulic vibration technology, as well as the new electro-hydraulic digital control technology, etc. were presented [12, 13]. Many scholars have been seeking new control elements to satisfy specific engineering requirements. For example, Hao et al. [14] utilized rotary valve structure to increase the wave frequency of exciter, and applied it to coal industry, metallurgical industry, construction industry, etc. Ruan et al. [15] proposed a high frequency electro-hydraulic exciter with rotary valve and studied the frequency characteristic of electro-hydraulic exciter, high frequency signal acquisition and control of typical excited wave forms. Ren et al. [16] studied vibration waveforms excited by an electro-hydraulic exciter with a two-dimensional rotary valve theoretically and experimentally. Other similar progresses include equilibrium hydraulic rotary valve with high pressure, large flow and electro-hydraulic rotary valve studied at Zhejiang University [17, 18] and rotating shaft hydraulic rotary valve with good manufacturability designed by Marcus [19]. A fluid driven PWM valve based on a unidirectional rotary spool was presented, and it was found that the rotary valve reduced actuation power from a cubic dependence to a square dependence by eliminating motion reversals during transition [20]. Liu et al. [21, 22] designed a single stage rotary valve for application to high energy and variable-frequency vibration condition. The single stage rotary valve can be used

to obtain the required vibration frequency and waveform by controlling the rotary velocity of spool, and thus meet different working requirements of tamping device.

In this paper, to make it easier to generate waves and improve wave amplitude in a certain plate frequency range, a simple push-type wave generating method using digital rotary valve control was proposed [23] and developed, and the control system model was established, and different wave amplitudes and lengths were generated and further analyzed.

2 Working Principle and Test Rig

The working principle of the novel digital rotary valve-controlled cylinder system is shown in Figure 1. It is composed mainly of a double-acting hydraulic servo cylinder, a digital rotary valve, an electro-hydraulic proportional axial variable piston pump, and a proportional relief valve. The wave experiment rig, as shown in Figure 1, includes a water tank (0.6 m wide×1.2 m high×12 m long), an electro-hydraulic control system, a wave generation mechanism and a wave height meter.

The working principle and structure of the designed rotary valve are shown in Figure 2. It can be seen that 4 shoulders with same structure are designed and manufactured on the rotary valve spool. The rotary frequency of the spool can be controlled by a servo motor, and the axial displacement of the spool can be controlled by a linear stepper motor, thus the opening of the spool as well as the flow through the opening can be controlled. The valve ports are designed symmetrical, so that the opening area of the valve ports on the front shoulder 1 can change from zero to the maximum, and from the maximum to zero, then so can the opening area of the corresponding valve ports on the nearby shoulder 4 do. On the other hand, when one valve port is closed, another valve port
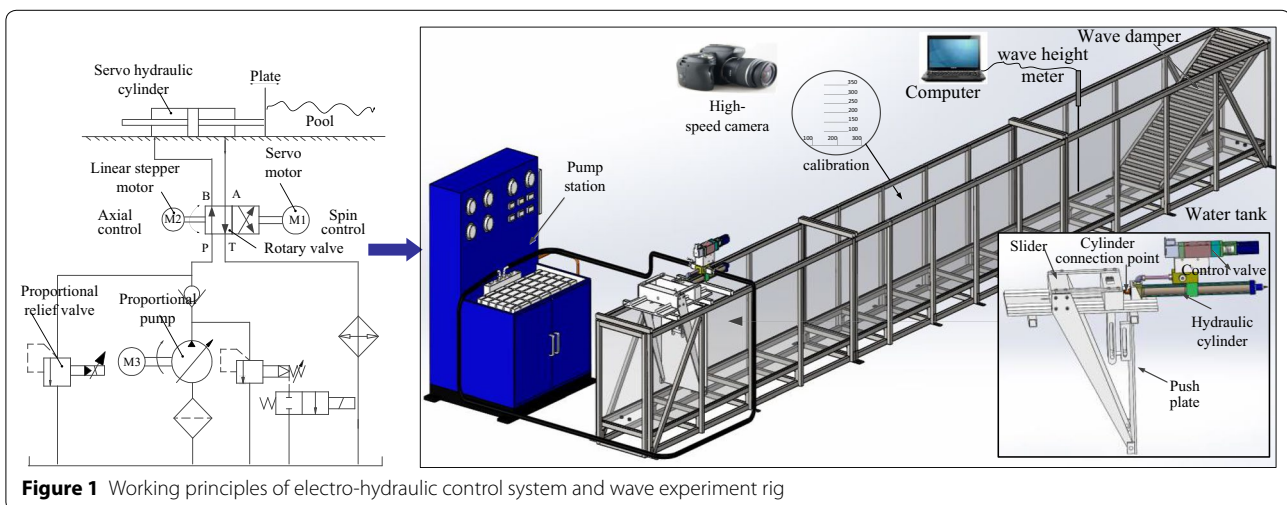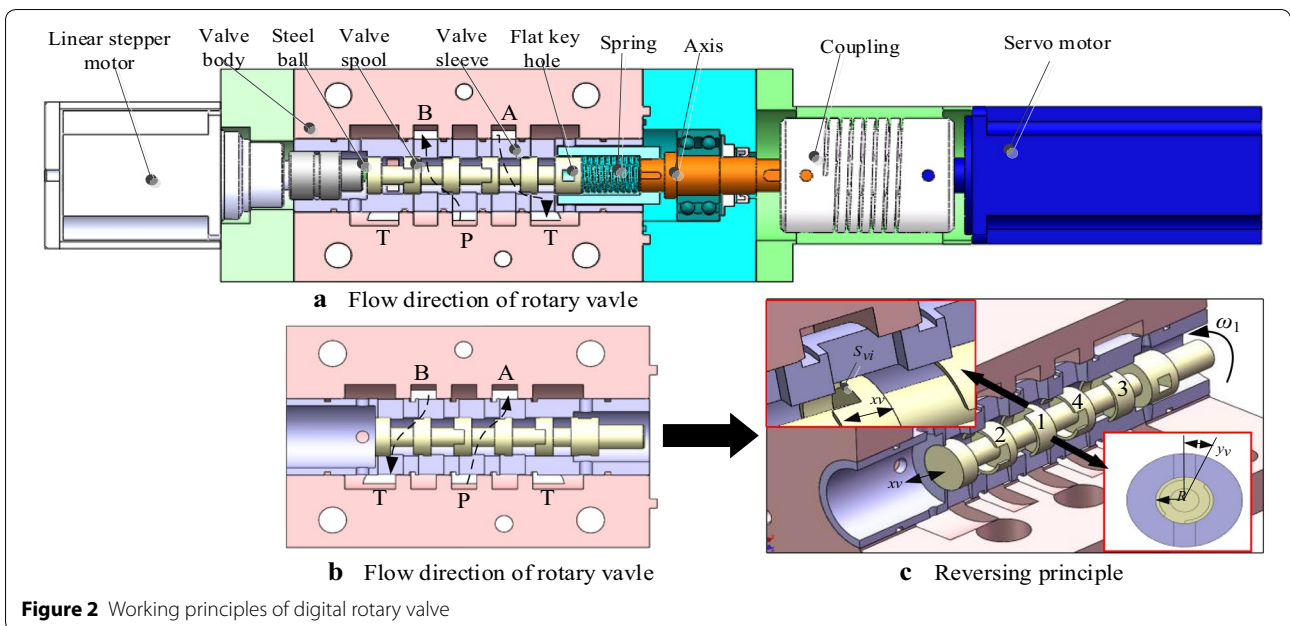

Figure 1 Working principles of electro-hydraulic control system and wave experiment rig

Liu *et al. Chin. J. Mech. Eng.*　　(2020) 33:5

Page 3 of 11

Figure 2 Working principles of digital rotary valve

on the opposite side of the same shoulder is just open, keeping the valve on working order.

When the valve core rotates to the specific angle as shown in Figure 2(a), oil flows from port P to port B, and then from port A to port T. In this case, the cylinder moves to the right. When the valve core rotates to another angle as shown in Figure 2(b), oil flows from P to A, and then from B to T, driving the cylinder to the left. With the change of servo motor's speed, the frequency of the rotary valve core changes, leading to the change of wave maker's working frequency. To meet higher flow for cylinder motion, linear flow and pressure control requirements, grooves in the valve core and windows in the sleeve are designed to be rectangular accordingly.

A test rig of wave experiment was established to validate the new working principle. By adjusting the stepper motor and the servo motor, we can control the axial displacement and the rotational speed of valve core respectively. Supply oil pressure can be set through the proportional relief valve. Consequently, the amplitude of wave plate becomes adjustable and the frequency of wave plate changeable. The experimental instruments are shown in Table 1. The main parameters of the new wave maker system are listed in Table 2. The operation parameters with instruments are listed in Table 3.

3 Mathematical Modelling
According to the Figure 1, the hydraulic transmission model is shown in Figure 3. The bottom of water tank is smooth and the hydrostatic depth is *d*. In the distal wave trough, there is no reflection, wave completely absorbed

Table 1 Experimental instruments

Instruments	Model (manufacturer)	Range
Proportional pump	A10VSO28DR/31RPPA12N00 (Rexroth)	40 L/min
Servo motor	ECMA-C20604R8 (Delta)	0–3000 r/min
Servo motor drive	ASD-B2-0421-B (Delta)	0–250 Hz
Linear stepper motor	57M42-12-002 (Haydon)	150–890 N
Stepper motor driver	DCM4010 (Haydon)	0–100 kHz
Servo hydraulic cylinder	CKM/20-40/28×200-N004-V (Atos)	0–200 mm
Proportional relief valve	DBE10-30B/315XY (Huadehydraulic)	0–31.5 MPa
Industrial Personal Computer (IPC)	DVP-06XA	0–20 mA
Pressure sensor	P200HGB250BM20M4B (Banna)	0–31.5 MPa
Displacement sensor	EHM0220MD341V01 (MTS)	0–220 mm
Wave height meter	YWH200-DXX (Chengdu autel)	0–1000 mm

Liu *et al. Chin. J. Mech. Eng.* (2020) 33:5

Page 4 of 11

Table 2 Main parameters of new wave maker system

Item	Value
Diameter of cylinder (D_0)	40 mm
Diameter of piston rod (d_0)	28 mm
Volume of cylinder (V_t)	1.28×10^{-4} m^3
Effective action area of hydraulic cylinder (A_p)	6.4×10^{-4} m^2
Axial opening width of rotary valve (x_v)	0–4 mm
Maximum Circumferential width of rotary valve (y_{vmax})	6.1 mm
Radius of the spool shoulder (R)	8 mm
Number of grooves on a single spool (Z)	2
Oil supply pressure (p_s)	0–8 MPa
Maximum flow (q_{smax})	40 L/min
Equivalent mass of wave plate (m_t)	30 kg
Depth of water (d)	400 mm
Flow rate coefficient (C_d)	0.62
Oil density (ρ)	870 kg/m^3
Effective bulk modulus of oil (β_e)	8×10^8 Pa
Density of water	1000 kg/m^3
Temperature of water	20 ℃

Table 3 Operation parameters with instruments

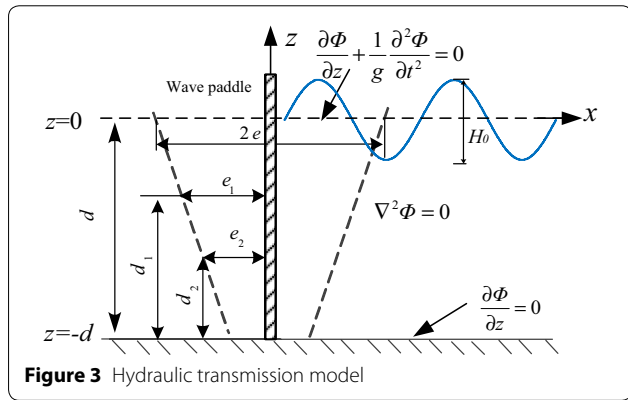| Operation parameter	Value	Instruments
x_v	0–4 mm	Stepper motor
n (f_j)	0–60 r/min (1–2 Hz)	Servo motor
p_s	0–2 MPa	Proportional relief valve

Figure 3 Hydraulic transmission model

by the wave damper. Assume that the wave propagation direction is the positive x axis, the vertical direction is the positive z axis, the origin of the coordinate is on the surface of the water. The wave amplitude is much less than the wave length. Φ is the velocity potential function. The boundary value problem for the wave maker in the wave

Table 4 Corresponding parameters of hydraulic transmission

f_j (Hz)	k	T_1
1	4.3	1.54
1.6	10.3	2.00
2	16.1	2.00

tank follows directly from the boundary value problem for two-dimensional waves propagating in an inviscid, incompressible, irrotational fluid. Boundary value problem specification for periodic water waves is shown in Figure 3. According to the above assumptions, the potential flow theory and small amplitude wave theory [24–26], the equation of wave amplitude of the front plate a0 and plate amplitude e in different cycles is expressed as follows:

$$
\begin{aligned}
T(\omega, d) = \frac{a_0}{e_1} = \frac{H_0}{2e_1} &= \frac{4\sinh kd}{\sinh 2kd + 2kd} \\
&\times \left(\frac{1 - e_2/e_1}{1 - d_2/d_1} \frac{d}{d_1} \sinh kd + \frac{e_2/e_1 - d_2/d_1}{1 - d_2/d_1} \sinh kd \right. \\
&\left. + \frac{1 - e_2/e_1}{1 - d_2/d_1} \frac{1}{kd_1} - \frac{1}{kd_1} \frac{1 - e_2/e_1}{1 - d_2/d_1} \cosh kd \right),
\end{aligned}
\tag{1}
$$

where H_0 is the wave height, d is the depth of water, e_1, e_2 are the amplitudes of plate motion distance from the bottom d_1, d_2, respectively, e is the amplitude of plate motion at water surface.

For push-type wave maker, $e_1 = e_2 = e, d_1 = d, d_2 = 0$. According to the cylinder connection point of Figure 1, e (namely, the amplitude of wave plate) is equal to the motion displacement of hydraulic cylinder y_p, so:

$$
T_1(\omega, d) = \frac{a_0}{e} = \frac{a_0}{y_p} = \frac{H_0}{2y_p} = \frac{4 \sinh^2 kd}{2kd + \sinh 2kd}.
\tag{2}
$$

The relation of the wave number k and the angular velocity of wave ω meets the dispersion formula: $\omega^2 = 4\pi^2 f_j^2 = gk\tanh(kd)$ [1], where f_j is the working frequency of the wave plate, namely the hydraulic cylinder working frequency. k cannot be directly obtained from the above formula, where k can be solved by means of Matlab software tool . The parameter values of k and T_1 used in the calculation are listed in Table 4.

The equivalent bridge of the rotary valve-controlled cylinder system is shown in Figure 4. It is assumed that the system pressure p_s is constant, the total supply flow is q_s, q_L is the flow through the load and p_L is the pressure drop across the load.

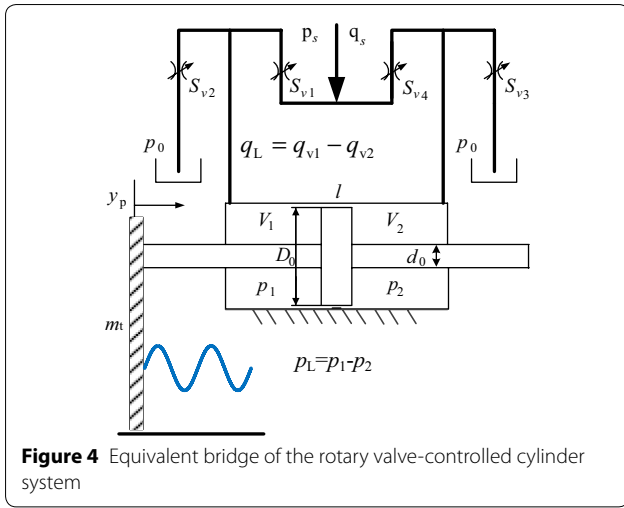The equations of flow through the orifices 1, 2, 3 and 4 are expressed as follows:

Liu *et al.* Chin. J. Mech. Eng.   (2020) 33:5

Page 5 of 11

Figure 4 Equivalent bridge of the rotary valve-controlled cylinder system

$$q_{v1} = C_d S_{v1} \sqrt{\frac{2(p_s - p_1)}{\rho}}, \tag{3}$$

$$q_{v2} = C_d S_{v2} \sqrt{\frac{2(p_1 - p_0)}{\rho}}, \tag{4}$$

$$q_{v3} = C_d S_{v3} \sqrt{\frac{2(p_2 - p_0)}{\rho}}, \tag{5}$$

$$q_{v4} = C_d S_{v4} \sqrt{\frac{2(p_s - p_2)}{\rho}}, \tag{6}$$

where p_1 and p_2 are the pressure of hydraulic cylinder two cavity respectively, C_d is the flow rate coefficient, ρ is the oil density, and S_{vi} ($i=1, 2, 3, 4$) are orifice area of valve ports on the correspondent shoulder i.

Firstly, it is assumed that the connecting pipeline between rotary valve and hydraulic cylinder is short, thick and symmetrical enough, the dynamic loss and the pressure loss of the pipe can be ignored, the oil temperature and bulk modulus of hydraulic oil are constant, and the leakage of hydraulic cylinder is zero. When the cylinder moves to the right, the flow rate continuity equations of the chamber of the cylinder can be used.

The left chamber is

$$q_{v1} - q_{v2} = \frac{dy_p}{dt} A_p + \frac{V_1}{\beta_e} \frac{dp_1}{dt}, \tag{7}$$

whereas the right chamber is

$$q_{v3} - q_{v4} = \frac{dy_p}{dt} A_p - \frac{V_2}{\beta_e} \frac{dp_2}{dt}, \tag{8}$$

where V_1 is the volume of forward chamber, $V_1 = V_{o1} + A_p y_p$, V_{o1} is the initial volume of forward chamber, V_2 is the volume of return chamber, $V_2 = V_t - (V_{o1} + A_p y_p)$, V_t is the total volume of cylinder chambers, β_e is the effective bulk modulus of oil and is assumed to be as constant in Low pressure test, A_p is the area of piston.

As the orifices are both matched and symmetrical, the flows in diagonally opposite arms of the bridge, as shown in Figure 4, are equal. Therefore, $S_{v1}(\theta) = S_{v3}(\theta + \pi)$, $S_{v4}(\theta) = S_{v2}(\theta + \pi)$.

The equations of the flow through the orifices in a cycle are expressed as follows:

$$\begin{cases} q_{v1} = q_{v3} = C_d S_{v1} \sqrt{\dfrac{2(p_s - p_1)}{\rho}} \\ \qquad = C_d S_{v3} \sqrt{\dfrac{2(p_2 - p_0)}{\rho}}, \quad (\pi - \theta \geq 0), \\ q_{v2} = q_{v4} = 0, \end{cases} \tag{9}$$

$$\begin{cases} q_{v1} = q_{v3} = 0, \\ q_{v2} = q_{v4} \\ \qquad = C_d S_{v2} \sqrt{\dfrac{2(p_1 - p_0)}{\rho}} \\ \qquad = C_d S_{v4} \sqrt{\dfrac{2(p_s - p_2)}{\rho}}, \\ \qquad\qquad (\pi - \theta \leq 0). \end{cases} \tag{10}$$

If the external leakage and internal leakage are zero, and $p_s = p_1 + p_2$, $p_L = p_1 - p_2$, the load flow of the cylinder is $q_L = q_{v1} - q_{v2}$. That is,

$$q_L = \text{sign}(\pi - \theta) \frac{C_d S_{vi}}{\sqrt{\rho}} \sqrt{p_s - \text{sign}(\pi - \theta) p_L}$$

$$= \begin{cases} C_d S_{v1} \sqrt{\dfrac{p_s - p_L}{\rho}}, & \pi - \theta \geq 0, \\ -C_d S_{v2} \sqrt{\dfrac{p_s + p_L}{\rho}}, & \pi - \theta \leq 0. \end{cases} \tag{11}$$

The total open area is $S_{vi} = 2x_v y_{vi}$, where x_v is the axial opening width of the valve.

It is assumed that the opening circumferential conduction width of B and A are y_{v1} and y_{v4}, respectively. If y_{v1} is from zero to the maximum, then from the maximum to zero, after that, to enter the next opening port of nearby shoulder subsequently, y_{v4} is also from zero

Liu *et al. Chin. J. Mech. Eng.* (2020) 33:5

Page 6 of 11

to the maximum, then from the maximum to zero, so the equations of y_{v1} and y_{v4} are:

$$y_{v1} = \begin{cases} 2R\sin\dfrac{\omega_1 t}{2}, 0 \le \omega_1 t < \dfrac{\pi}{4}, \\ 2R\sin\left[\dfrac{\pi}{4} - \dfrac{\omega_1 t}{2}\right], \dfrac{\pi}{4} \le \omega_1 t < \dfrac{\pi}{2}, \\ 0, \dfrac{\pi}{2} \le \omega_1 t < \dfrac{3\pi}{4}, \\ 0, \dfrac{3\pi}{4} \le \omega_1 t \le \pi, \end{cases} \quad (12)$$

$$y_{v4} = \begin{cases} 0, 0 \le \omega_1 t < \dfrac{\pi}{4}, \\ 0, \dfrac{\pi}{4} \le \omega_1 t < \dfrac{\pi}{2}, \\ 2R\sin\left[\dfrac{\omega_1 t}{2} - \dfrac{\pi}{4}\right], \dfrac{\pi}{2} \le \omega_1 t < \dfrac{3\pi}{4}, \\ 2R\sin\left[\dfrac{\pi}{2} - \dfrac{\omega_1 t}{2}\right], \dfrac{3\pi}{4} \le \omega_1 t < \pi, \end{cases} \quad (13)$$

where R is the radius of the spool shoulder, f is the rotational frequency of spool, and ω_1 is the rotational angular velocity of valve spool.

Figure 2 shows that a single complete cycle of spool and the twice of oil reversing make hydraulic cylinder oscillating back and forth twice, so the relation between the working frequency of hydraulic cylinder and the rotational frequency of spool is $f_j = 2f$.

The equation of motion for the cylinder is

$$A_P(p_1 - p_2) = m_t\ddot{y}_p + B_c\dot{y}_p + F_L. \quad (14)$$

where m_t is the equivalent mass, B_c is the total damping coefficient, and F_L is the force by the action of water on the plate. The system is greatly affected by the mass inertial force and the force by the action of water on the plate, the effect of other forces are so little that can be neglected when conducting actual calculation.

The wavefront equation of the two-dimensional small amplitude propulsion wave with constant depth is

$$\eta = a_0\cos\theta = a_0\cos(kx - \omega t), \quad (15)$$

where θ is the phase of the wave. The determination of the constants k and ω is as follows:

(1) When x is increased or decreased by one wave length L, the wavefront height η should be constant. This must make

$$kL = 2\pi. \quad (16)$$

(2) When the time increments by one cycle T, the wave surface height of the same point should be constant, that is

$$\omega T = 2\pi. \quad (17)$$

Based on the above dispersion formula: $\omega^2 = gk\tanh(kd)$ [1], substitute into Eqs. (16) and (17), so:

$$L = \frac{gT^2}{2\pi}\tanh kd. \quad (18)$$

The relation between the working frequency of hydraulic cylinder and the rotational frequency of spool is $f_j = 2f$, so: $T = 1/f_j = 1/2f$.

4 Theoretical and Experimental Results

Figure 5 show the wave experiment and acquisition interface system of wave height meter. The distance between the wave height meter is X, the time difference of initial wave height data is Δt. We can get L from the equation $L = X/\Delta t f_j$ with the experimental data.

Test values in the wave experiment were compared with those obtained in the numerical analysis. It was assumed that the initial point of cylinder piston is in the middle with the maximum opening of valve port, and the cylinder to the right direction is positive to correspond to the hydraulic transmission model. The main factors and the control parameters for wave experiment can be obtained by continuously adjusting different input parameters (x_v, p_s and f_j), and analyzing output curves (y_p, L and a_0) in the solution process of mathematical models by means of Simulink software tool.

In the actual operation, because no feedbacks were used in the hydraulic control system, the cylinder piston rod was set to the leftmost position in each experiment and the valve port was set to closed at the same time. Therefore, the motion displacement of hydraulic cylinder in a cycle was $2y_p$. The wave height H_0 ($2a_{0max}$) of experimental data was measured by the wave height meter.
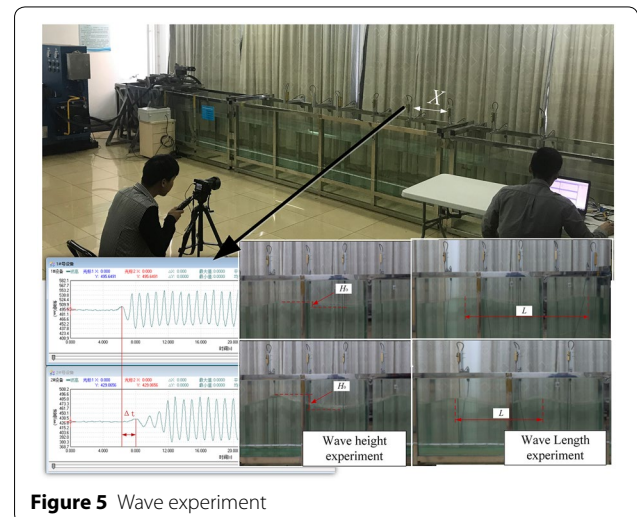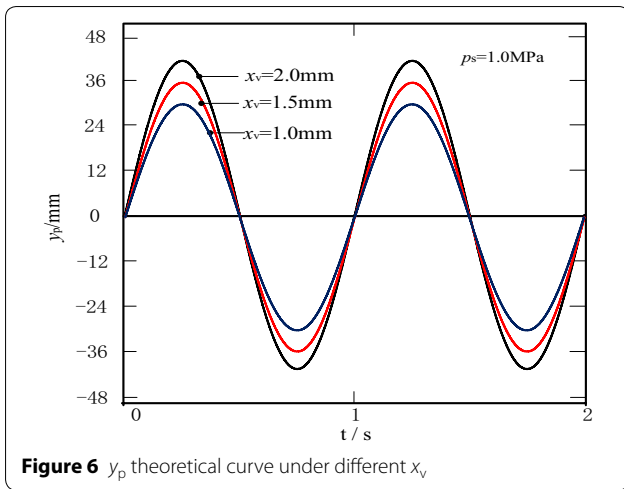

Figure 5 Wave experiment

Figure 6 y_p theoretical curve under different x_v

4.1 Influence of Different x_v and f_j on Wave Simulation

Figure 6 and Figure 7(a) show the y_p-t and a_0-t curves under different x_v at the working frequency of 1 Hz. From equation $S=2x_vy_{vi}$, Figure 6 and Figure 7(a), S_v is determined by x_v, directly affecting y_p and a_0, Thus, x_v is the crucial factor for the motion amplitude of hydraulic cylinder and wave amplitude, and the bigger x_v is, the bigger S_v, y_p and a_0 will be. Under the condition of 1.0 MPa (oil supply pressure), 1 Hz (Plate motion frequency, $T_1=1.54$), 2.0 mm (Axial opening width), the maximum wave amplitude can reach to 64 mm. It can be seen from Figure 6 and Table 5 that test value and theoretical value in the maximum wave amplitude a_{0max} agree relatively well.

Figure 7(b) shows a_0 and y_p under different work frequencies at 1.0 MPa oil supply pressure. From Figure 7(b), it can be seen that when work frequency is 1.6 Hz ($T_1=2$), the maximum amplitude of the cylinder is 16 mm (x_v is set to 1 mm) or 21 mm (x_v is set to 2 mm), and
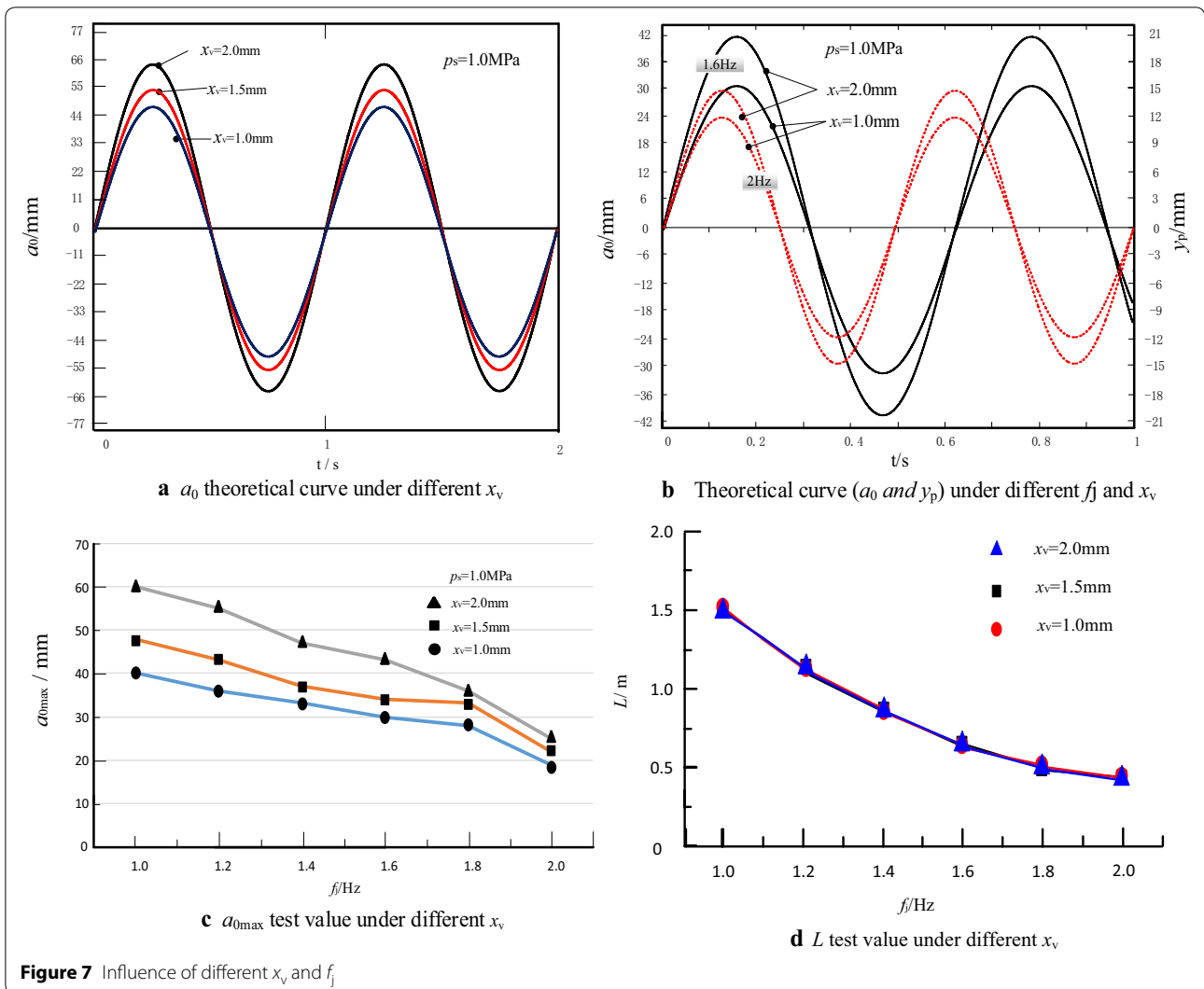

a a_0 theoretical curve under different x_v

b Theoretical curve (a_0 *and* y_p) under different f_j and x_v

c a_{0max} test value under different x_v

d L test value under different x_v

Figure 7 Influence of different x_v and f_j

Liu *et al. Chin. J. Mech. Eng.*   (2020) 33:5

Page 8 of 11

Table 5 Main comparison between theoretical and test values of a_{0max} (L) (p_s = 1 MPa) (mm)

f (Hz)	x_v					
	1 mm		1.5 mm		2 mm	
	Theoretical results	Test results	Theoretical results	Test results	Theoretical results	Test results
1	48 (151)	40 (150)	55 (151)	48 (154)	64 (151)	60 (154)
1.6	32 (61)	30 (62)	36 (61)	33 (62)	42 (61)	45 (63)
2	24 (39)	19 (41)	27 (39)	23 (41)	30 (39)	26 (40)

a_{0max} is 32 mm (x_v is set to 1 mm) or 42 mm (x_v is set to 2 mm). When work frequency is 2 Hz ($T_1 = 2$), the maximum amplitude of the cylinder is 12 mm (x_v is set to 1 mm) or 15 mm (x_v is set to 2 mm), and a_{0max} is 24 mm (x_v is set to 1 mm) or 30 mm (x_v is set to 2 mm). It can be also drawn from the curve of different work frequencies that the value of a_0 can be determined by x_v. A larger value of x_v will lead to larger a_0.

Figure 7(c) shows the relationship between the working frequency and a_{0max} ($H_0/2$) under different x_v. The wave amplitude descends with the increase of the plate working frequency, the higher the working frequency, the smaller the wave amplitude. a_{01} (x_v is set to 2 mm) is higher than a_{02} (x_v is set to 1.5 mm), and a_{02} (x_v is set to 1.5 mm) is higher than a_{03} (x_v is set to 1 mm). The main comparison between theoretical and test values of a_{0max} under the same pressure are shown in Table 5. The test results under different x_v are in accordance with the theoretical calculation results, but the test values are slightly lower than the theoretical values.

Figure 7(d) shows the relationship between the working frequency and L under different x_v. The wave length descends with the increase of the plate working frequency, the higher the working frequency, the smaller the wave length. At the same frequency, the wave length remains unchanged with the axial opening width change. The main comparison between theoretical and test values of L under the same pressure are shown in Table 5. The test results under different x_v are in accordance with the theoretical calculation results.

4.2 Influence of Different p_s and f_j on Wave Simulation

Figure 8(a) shows y_p and a_0 curves under different oil supply pressure. It can be seen from Figure 8(a), when f_j is set to 1 Hz, x_v is set to 1 mm, the maximum amplitude of the cylinder can reach to 25 mm under the pressure of 0.9 MPa, 31 mm under the pressure of 1.0 MPa, 36 mm under the pressure of 1.2 MPa, and a_{0max} can reach to 39 mm under the pressure of 0.9 MPa, 48 mm under the pressure of 1.0 MPa, 55 mm under the pressure of 1.2 MPa. Numerical curve shows that a_0 can be controlled by the oil supply pressure. The higher the oil supply pressure, the larger the wave plate amplitudes and wave amplitudes. It can be seen from Figure 8 and Table 6 that test value and theoretical value in the maximum wave amplitude agree relatively well.

Figure 8(b) shows a_0 at different work frequencies when x_v is set to 1 mm. It can be seen from the Figure 8(b) that when the work frequency is 1.6 Hz ($T_1 = 2$), the maximum amplitude of the cylinder is 15 mm (p_s is set to 1.0 MPa) or 18 mm (p_s is set to 1.2 MPa), and a_{0max} is 30 mm (p_s is set to 1.0 MPa) or 36 mm (p_s is set to 1.2 MPa). When the work frequency is 2 Hz ($T_1 = 2$), the maximum amplitude of the cylinder is 12 mm (p_s is set to 1.0 MPa) or 14 mm (p_s is set to 1.2 MPa), and a_{0max} is 24 mm (p_s is set to 1.0 MPa) or 28 mm (p_s is set to 1.2 MPa). It can be also drawn from the curve of different work frequencies that the value of a_0 can be determined by p_s. The higher the p_s, the greater the a_0.

Figure 8(c) shows the relationship between the working frequency and the a_{0max} ($H_0/2$) under different supply pressure. a_{01} (p_s is set to 1.2 MPa) is higher than a_{02} (p_s is set to 1.0 MPa). The test results under different p_s are in accordance with the theoretical calculation results. It can be seen from Figure 7(c) and Figure 8(c), a_0 descends with the increasing of working frequency. The main comparison between theoretical and test values of a_{0max} under the same x_v are shown in Table 6. Test values are slightly lower than the theoretical values. The differences between the test and theoretical values in Table 5 and Table 6 are mainly caused by water leaks from the gaps at both sides of the wave paddle.

Figure 8(d) shows the relationship between the working frequency and L under different supply pressure. At the same frequency, the wave length remains unchanged with the supply pressure change. The main comparison between theoretical and test values of L under the same x_v are shown in Table 6. The test results under different supply pressure are in accordance with the theoretical calculation results.

5 Conclusions

The experiment and analysis results show that the motion frequency and amplitude of push-type wave maker can be continuously adjusted and the various required regular waves can be obtained conveniently.
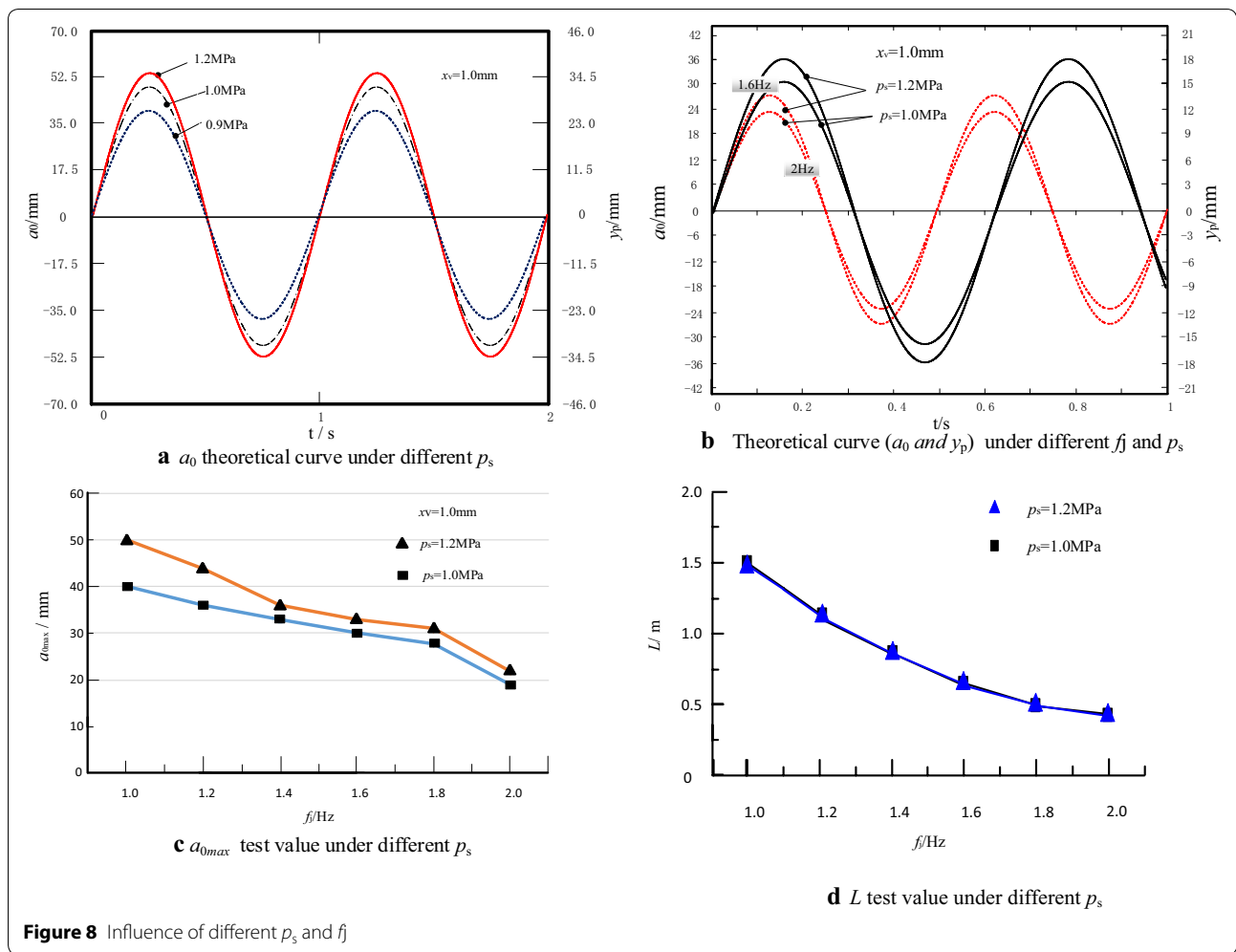
a a_0 theoretical curve under different p_s

b Theoretical curve (a_0 *and* y_p) under different fj and p_s

c a_{0max} test value under different p_s

d L test value under different p_s

Figure 8 Influence of different p_s and fj

Table 6 Main comparison between theoretical and test values of a_{0max} (L) ($x_v = 1$ mm) (mm)

f (Hz)	p_s			
	1 MPa		1.2 MPa	
	Theoretical results	Test results	Theoretical results	Test results
1	48 (151)	40 (150)	55 (151)	50 (149)
1.6	32 (61)	30 (62)	37 (61)	34 (62)
2	24 (39)	19 (41)	28 (39)	23 (42)

The axial opening width of the valve is the crucial factor for the plate amplitude and the wave amplitude. A larger value of the axial opening width lead to larger the wave plate amplitude and wave amplitude. The wave amplitude also depends on oil supply pressure, the higher the oil supply pressure, the greater the plate amplitude and the wave amplitude. At the same water depth, the working frequency of push plate determines wave number and wave length. Wave length is not affected by the axial opening width and the oil supply pressure. Although the wave amplitude and length descends with the increase of the working frequency, the wave amplitude can be easily improved by setting the axial opening width of the valve and the oil supply pressure of the system. These results indicate that different regular waves can be obtained conveniently by the new wave generating method, and the wave amplitude can be further improved in a certain plate frequency range. These facilitate convenient implementation of wave experiment. Based on the characteristics of high power electro-hydraulic system, the new approach demonstrates its potential application to achieve high-power wave experiment with high-power wave maker system.

Considering the feasibility and practicability of the rotary valve-controlled cylinder system applied to high-power wave experiment, future efforts will focus on practical application of the high-power wave maker. Future

work includes vibration cylinder bias compensation with feedbacks, optimized and integrated design of the device.

List of symbols

A_p: Area of piston; a_0: Wave amplitude; B_c: Total damping coefficient; C_d: Flow rate coefficient; d: Depth of water; e: Amplitude of wave plate (water surface); e_1: Amplitude of plate distancing from the bottom d_1; e_2: Amplitude of plate distancing from the bottom d_2; F_L: Force by the action of water on the plate; f: Rotary frequency of spool; f_j: Working frequency of the wave plate; g: Gravitational acceleration; H_0: Wave height ($2a_0$); k: Wave number; L: Wave length; m_t: Equivalent mass; p_L: Pressure drop across the load; p_1, p_2: Pressure of hydraulic cylinder two cavity; p_s: System pressure; q_s: Total supply flow; q_L: Flow through load; R: Radius of spool shoulder; T: Ratio of wave amplitude and paddle amplitude; S_i: Orifice area of different valve ports; V_1: Volume of forward chamber; V_2: Volume of return chamber; V_{o1}: Initial volume of forward chamber; V_t: Total volume of cylinder chamber; x_v: Axial opening width of valve; y_p: Amplitude of wave plate (hydraulic cylinder); y_{vi}: Opening circumferential conduction width; β_e: Effective bulk modulus of oil; ρ: Oil density; ω: Angular velocity of wave; ω_1: Rotational angular velocity of valve spool; Φ: Velocity potential function.

Authors' contributions

YL was in charge of the whole trial; JZ wrote the manuscript; RS and JC determined the subject discussed and wrote an outline; QX and FH assisted with revision and translation. All authors read and approved the final manuscript.

Authors' Information

Yi Liu, received his PhD degree in mechanical engineering from *Zhejiang University, China*, in 2013. Since 2013, he has been an associate professor with *Zhejiang University, Ningbo Institute of Technology*. His current research interests include electro-hydraulic control systems of vibration exciters and mechatronic systems design.

Jiafei Zheng, received the bachelor degree in machine design manufacture and automation from *Ningbo Institute of Technology, Zhejiang University, China*, in 2018. She became a graduate student with *Soochow University, China*. Her current research interests include wave simulation control, controlling and optimizing of the complex system, development of production management information system.

Ruiyin Song, born in 1974, is currently an associate professor at *Ningbo Institute of Technology, Zhejiang University, China*. He received his PhD degree from *Zhejiang University, China*, in 2006. His research interests include wave energy generation technology and wave simulation control.

Qiaoning Xu, received the PhD degree in mechanical engineering from *Zhejiang University, China*, in 2015. Since 2015, she has been in *Zhejiang University of Technology, China*. Her current research interests include fault diagnosis for hydraulic systems and electro-hydraulic system control.

Junhua Chen, received his Ph.D. degree in mechanical engineering from *Nanchang University, China*, in 2011. Since 2018, He was the Vice Chairman of *Ningbo Mechanical Engineering Society*. His current research interests include marine equipment and mechatronics.

Fangping Huang, received his Master's degree in mechanical engineering from *Zhejiang University, China*, in 2005. Since 2010, he has been an associate professor with *Ningbo Institute of Technology, Zhejiang University*. His current research interests include electro-hydraulic control systems and mechatronic systems design.

Competing interests
The authors declare that they have no competing interests.

Author Details
[1] Ningbo Institute of Technology, Zhejiang University, Ningbo 315100, China. [2] Ningbo Research Institute, Zhejiang University, Ningbo 315100, China. [3] Soochow University, Suzhou 215000, China. [4] Zhejiang University of Technology, Hangzhou 310023, China.

References

[1] R Dean, R Darymple. Water wave mechanics for engineers and scientists. *World Scientific*, 1991.
[2] H A Schaffer. Second-order wave maker theory for irregular waves. *Ocean Engineering*, 1996, 23(1): 47-88.
[3] C E Synolakis. Generation of long waves in laboratory. *Journal of Waterway, Port, Coastal, and Ocean Engineering*, 1990, 166(2): 252-266.
[4] D G Goring. Tsunamis—The propagation of long waves onto a shelf. Pasadena, California: California Institute of Technology, 1979.
[5] A Moronkeji. Physical modelling of tsunami induced sediment transport and scour. *Proceedings of the 2007 Earthquake Engineering Symposium for Young Researchers*, 2007.
[6] M H Teng, K Feng, T I Liao. Experimental study on long wave run-up on plane beaches. *Proceeding of the Tenth International Offshore and Polar Engineering Conference*, Seattle, USA, 2000: 660-664.
[7] N J Wu, S C Hsiao, H H Chen, et al. The study on solitary waves generated by a piston-type wave maker. *Ocean Engineering*, 2016, 117(1): 114-129.
[8] N J Wu, T K Tsay, Y Y Chen. Generation of stable solitary waves by a piston-type wave maker. *Wave Motion*, 2014, 51(2): 240-255.
[9] H W Li, Y J Pang, Z Sun. Simulation of white noise irregular wave and focused wave in ocean basin. *Huazhong University of Science and Technology*, 2013, 41(1): 89-92.
[10] G SHEN, Z C ZHU, W D ZHU, et al. Real-time tracking control of electro-hydraulic force servo systems using offline feedback control and adaptive control. *ISA Transactions*, 2017, 67: 356-370.
[11] G Shen, Z C Zhu, X Li, et al. Real-time electro-hydraulic hybrid system for structural testing subjected to vibration and force loading. *Mechatronics*, 2016, 33: 49-70.
[12] Y Ren, X C Ji, J Ruan. Output characteristics of a horizontal type electro-hydraulic excitation system with inertial loading: Modeling and experimentation. *Journal of Mechanical Science and Technology*, 2019, 33(11): 5157-5167.
[13] Y Ren, H S Tang, J W Xiang. Experimental and numerical investigations of hydraulic resonance characteristics of the high-frequency excitation system. *Mechanical System and Signal Processing*, 2019, 131: 617-632.
[14] J G Hao, Y C Zhang. Study on the properties of a new electro-hydraulic exciting system. *Journal of Taiyuan University of Technology*, 2003, 6: 706-709.
[15] W R Li, J Ruan, Y Ren, et al. Research on low-frequency characteristics of one-pole vibration cylinder controlled by 2D valve. *Proc. 8th ICFP*, 2013: 188-192.
[16] Y Ren, J Ruan. Theoretical and experimental investigation of vibration waveforms excited by an electro-hydraulic type exciter for fatigue with a two-dimensional rotary valve. *Mechatronics*, 2016, 33: 161-172.
[17] J Cui, F Ding, Q P Li. Novel bidirectional rotary proportional actuator for electro-hydraulic rotary valves. *IEEE Transactions on Magnetics*, 2007, 43(7): 3254-3258.
[18] J Cui, F Ding, Q P Li. Static torque characteristics of high-pressure bidirectional rotary proportional solenoid. *Journal of Zhejiang University*, 2007, 41(9): 1578-1581.
[19] B L Marcus. Rotary servo valve. U.S. Patent 5954093, Sept. 21, 1999.
[20] H C Tu, M B Rannow, M Wang, et al. Design, modeling, and validation of a high-speed rotary pulse-width-modulation on/off hydraulic valve. *Journal of Dynamic Systems, Measurement and Control*, 2012, 134(11): 1-12.
[21] Y Liu, S K Cheng, G F Gong. Structure characteristics of valve port in the rotation-spool-type electro-hydraulic vibrator. *Journal of Vibration and Control*, 2017, 23(13): 2179-2189.

Liu *et al. Chin. J. Mech. Eng.*   (2020) 33:5

Page 11 of 11

[22] Y Liu, G F Gong, H Y Yang, et al. Regulating characteristics of new tamping device exciter controlled by rotary valve. *IEEE/ASME Transactions on Mechatronics*, 2016, 21(1): 497-505.

[23] Y Liu, S K Cheng, M J Zhu, et al. A wave machine based on hydraulic drive mode:China, 201410060768.8. 2014-05-21.

[24] J P Giesing. Two-dimensional potential flow theory for multiple bodies in small-amplitude motion. *AIAA Journal*, 2015, 8(11): 1944-1953.

[25] Q Zang, J Huang, Z Liang. Slosh suppression for infinite modes in a moving liquid container. *IEEE/ASME Trans. on Mechatoronics*, 2015, 20(1): 105-114.

[26] Y X Yu. *Random wave and its application in engineering*. Dalian: Dalian University of Technology Press, 2011.